Multitarget Physical Activities Monitoring and Classification Using a V-Band FMCW Radar

Victor G. Rizzi Varela, *Graduate Student Member, IEEE*, Davi V. Q. Rodrigues, *Graduate Student Member, IEEE*, Leya Zeng, *Graduate Student Member, IEEE*, and Changzhi Li, *Senior Member, IEEE*

***Abstract*— This work proposes a radar-based physical activities monitoring solution capable of detecting, classifying, and counting the number of repetitions of multiple human subjects doing different exercises simultaneously in front of the radar, using only one monostatic radar. Four exercises were performed in the experiments: sit-ups, push-ups, squats, and jump rope which are very common exercises performed in and out of the gym without the need for expensive gym equipment. A 60-GHz frequency-modulated continuous-wave (FMCW) radar was used in the experiments. The extracted data from the radar were processed using MATLAB R2021b, and the features were extracted using range–Doppler frames and micro-Doppler (mD) analysis generating a spectrogram. By combining these two analyses, information about the range, time, Doppler, and radar cross section (RCS) can be extracted for each individual. To validate the feasibility and robustness of the work in realistic scenarios, static and moving clutter were added to some of the measurements.**

***Index Terms*— Frequency-modulated continuous-wave (FMCW) radar, machine learning, multiple target detection, physical activities monitoring, range–Doppler, spectrogram, time–Doppler.**

I. Introduction

PHYSICAL activities may enhance health, reduce excess body fat, prevent many chronic diseases such as type 2 diabetes and some cancers, and can reduce symptoms of depression [1]. Exercise monitoring is crucial for high-performance athletes or people who frequently exercise to accomplish their goals. With the growing interest in achieving better performance in physical activities over the years, technologies have been developed to help monitor the movements aiming for fewer injuries and better gains. Examples of technologies applied to physical activities are accelerometers, gyroscopes, and camera-based systems [2], [3], [4], [5], [6]. In addition to the technologies cited, radars are one of the emerging solutions for human motion recognition. Portable microwave/millimeter-wave (mmWave) radars are noncontact devices that offer a noninvasive approach to human movement recognition while preventing privacy concerns associated with cameras and operate under any lighting conditions, including scenarios with abrupt changes in the illumination, and the required computational load during signal processing is considerably lower than the required by camera-based technologies. Vital signs detection, structural health monitoring, and nondestructive testing are examples of continuous-wave (CW) radar applications. By modulating the frequency of the radar wave, it is possible to also extract range information and enable a diverse range of new applications such as face recognition classification, shooter detection, human–vehicle classification, hand gesture recognition, fall detection, inattentive driving behavior detection, and vocal folds vibration detection which are some of the examples that have been widely studied [7], [8], [9], [10], [11], [12], [13], [14], [15].

Since frequency-modulated continuous-wave (FMCW) radars can provide Doppler and range information, some works with multiple targets have been proposed for vehicle applications, where the radar is located inside the vehicle, and several targets could be moving simultaneously. Efforts were made to extract and identify the correct combination of beat frequencies for multiple objects in the radar's field of view and distinguish ranges and velocities for each target with wide relative velocity and range [16], [17], [18], [19]. On the other hand, it is possible to extract 2-D position information by taking the advantage of two receiving antennas. With this, range and speed measurements of multiple targets moving in a scenario can be retrieved [20]. More examples of multiple target detection using beamforming are depicted in [15], where vocal folds vibration detection in a multitarget scenario is achieved using an FMCW with two TX and four RX antennas, and in [21], where an FMCW with multiple receiving antennas was used to detect the behavior of multiple patients in a hospital scenario. The classification was performed using a deep convolutional neural network (CNN), achieving an accuracy of approximately 80%.

Another interesting and emerging application is to detect human physical activities and classify the movements. For instance, an accelerometer sensor can be attached to the user's body, and the signal extracted during the free weight exercises can be utilized to collect classification features using long short-term memory (LSTM) neural networks from a single exercise [22]. Another example is to use the channel state information (CSI) embedded in Wi-Fi signals to retrieve information about exercises wirelessly, achieving

Manuscript received 26 August 2022; revised 15 October 2022; accepted 10 November 2022. Date of publication 9 December 2022; date of current version 18 January 2023. This work was supported by National Science Foundation (NSF) under Grant ECCS-2030094 and Grant ECCS-1808613. The Associate Editor coordinating the review process was Dr. Zhengyu Peng. *(Corresponding author: Victor G. Rizzi Varela.)*

The authors are with the Department of Electrical and Computer Engineering, Texas Tech University, Lubbock, TX 79409 USA (e-mail: vrizziva@ttu.edu; davi.rodrigues@ttu.edu; lezeng@ttu.edu; changzhi.li@ttu.edu).

Digital Object Identifier 10.1109/TIM.2022.3227998

a 93% classification accuracy using a deep neural network (DNN) [23]. A similar approach to this work using an FMCW radar is depicted using a multiple-channel system with two transmit and four receiving antennas, where physical activities were classified using CNNs [24]. However, for the past three examples, only one exercise was analyzed at a time. To analyze the robustness of physical activities data extraction using an FMCW radar, an experiment is reproduced in a scenario where one person was performing an exercise and was treated as the target of interest, while another person was doing exercises or moving behind the target, so interferences were added to the baseband data. After processing, the signal of interest was successfully recovered [25]. Another example of detecting multiple targets is shown in [26], where two human subjects performed exercises simultaneously in the radar's field of view. This time, two human subjects were treated as targets of interest, and both micro-Doppler (mD) signatures were recovered and analyzed. However, both studies were limited to a scenario where only two exercises at fixed ranges were performed in front of the radar, and the exercises carried out were exclusively sit-ups and push-ups. Furthermore, a feature extraction strategy for classifying the movements was not proposed.

This work investigates four different types of exercises performed in front of an mmWave radar in a scenario with potential moving and/or stationary clutters. Moreover, up to three exercises were carried out simultaneously as the targets of interest. A total of 20 different experimental layouts were recorded during data collection. In contrast to other works that analyze multiple simultaneous targets using complex multichannel systems [15], [20], [21], a strategy that uses only one receiving and one transmitting antenna was employed to reduce the signal complexity further. The exercises analyzed are sit-ups, push-ups, squats, and jump rope. Furthermore, a machine learning-based classification scheme is proposed by extracting features from mD signatures and range–Doppler frames.

For classification purposes, seven human subjects were recorded by performing the proposed exercises since different people perform exercises in different ways. The fixed-beam radar illuminated all subjects and potentially moving, and stationary clutters at all times. An approach to differentiate between human subjects exercising from possible clutters is presented. The features were fed into machine learning algorithms using tenfold cross-validation, and classification accuracy of 95% was achieved with the quadratic support vector machine (SVM).

The remainder of this article is organized as follows. Section II depicts the data processing and the theory behind multiple target detection and feature extraction. Then, the experiments performed are presented in Section III. Lastly, this article is concluded in Section IV.

II. Data Processing and Theory

A. Overview

An example of a scenario for one of the experiments using a 60-GHz FMCW radar is exhibited in Fig. 1. Multiple people (targets of interest) doing physical activities are simultaneously illuminated by the electromagnetic waves (EMs) transmitted by an mmWave FMCW radar. The human subjects performing the exercises will send a limited amount of energy back to the radar. The amount of energy reflected from the targets depends on the radar cross section (RCS), which is influenced by the size of the target relative to the wavelength of the signal, the absolute size of the target, the angle of the subject relative to the radar, the material of the target, and the polarization of the transmitted and received signals relative to the orientation of the target. Based on the received signal reflected from each target, data containing information about the exercises can be extracted and analyzed. On the other hand, Fig. 2 illustrates the mD signatures in a single range bin and the range–time profile extracted from all four exercises. Only one person placed 2 m away in front of the radar did the exercises. The radar system was positioned 0.5 m above the ground, and no clutters were included in the analysis. Fig. 2(a) illustrates the radar signatures associated with a person doing sit-ups. In the experiments, the subjects performed the sit-ups with their backs turned to the radar. The motion for this exercise is similar to a sinusoid; since the back is moving back and forth relative to the radar, the range with the maximum RCS also changes. Fig. 2(b) depicts the radar signatures associated with a person doing push-ups. The amplitude of the push-up movement is small compared to other types of exercises because it is made by bending half of the arm. Therefore, if the human subject is familiar with the exercise, it can be performed faster than sit-ups and squats; since the subject must be laid down, signatures of the head and other body parts can be seen in the range–time plot. Fig. 2(c) exhibits an example of the range profile and the spectrogram recorded from a person doing squats. This exercise has a similar signature compared to push-ups because there is not much range migration associated with them since the body moves mainly on the elevation angle. However, the reflected signals from a person doing squats also present strong mD signatures from the bending knee. The point of maximum RCS changes its range minimally for this exercise. Finally, Fig. 2(d) shows the signature of a jump rope movement. Since the human subject must jump, the range of maximum RCS might change over time depending on the subject's experience although it is supposed to be a stationary movement. For this exercise, the frequency of the

Fig. 1. Multitarget physical activities monitoring and classification scenario using a 60-GHz FMCW radar.

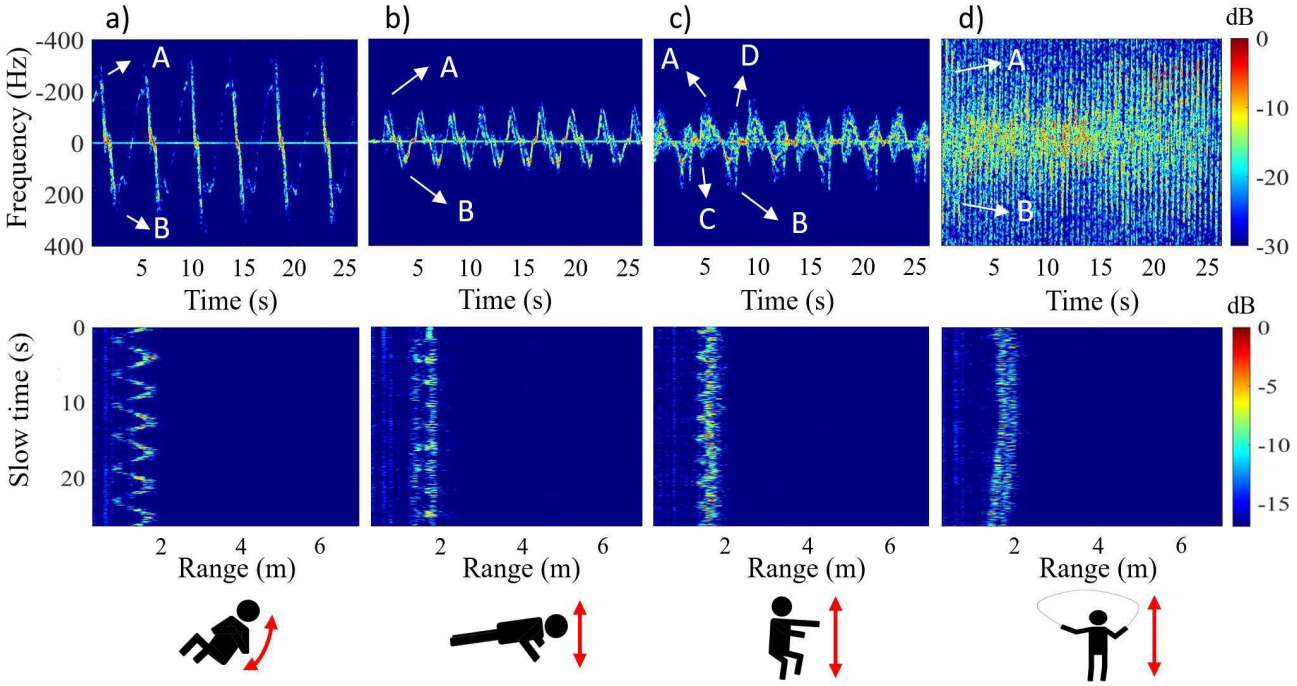

Fig. 2. Example of mD signatures and range–time analysis from one single exercise performed at 2 m away from the radar. Spectrogram and range–time of: (a) six sit-ups performed with the back turned to the radar, where A is the lying down movement and B is the going up movement; (b) eight push-ups, where A is the arm bending movement and B is the arm stretching movement; (c) six squats, where A is the sitting movement, B is the going up movement, and C and D represent the knee signatures of the movement; and (d) 51 jump rope repetitions, where A is the jump movement and B is the landing after a jump.

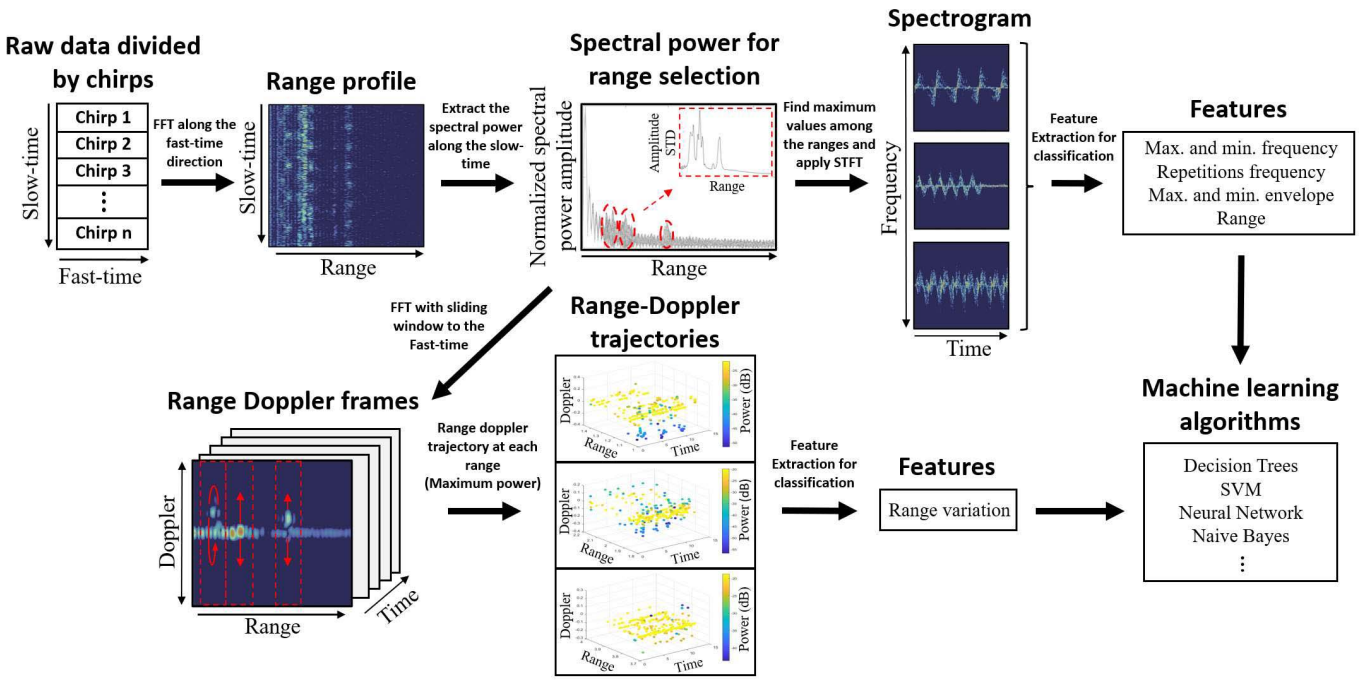

Fig. 3. Block diagram of the feature extraction for multiple exercises using mD signatures and range–Doppler frames.

movement is much higher than in the other three exercises, and the Doppler signatures are also high due to the jump motion being much faster. Another important point is that depending on the relative position between the radar and the illuminated targets of interest, the corresponding range–Doppler signatures and spectrograms will differ.

B. Data Processing

The block diagram of the feature extraction using a 60-GHz FMCW radar is detailed in Fig. 3. First, the raw baseband data extracted from the radar is divided into a matrix $\mathbf{B}(m, n)$, where $m = [1, 2, 3, \ldots, M]$ corresponds to the number of chirps and $n = [1, 2, 3, \ldots, N]$ is the number of samples

per chirp. The total time duration is called slow time, and the duration of each chirp is called fast time. To calculate the range profile, a fast Fourier transform (FFT) is applied to the fast-time dimension of the raw data matrix, generating a new matrix $\mathbf{R}(m, r)$, where r contains the range bins. The next step is to identify the range bins where each exercise is being performed and separate them from each other and from potentially stationary, and moving clutters since multiple exercises are being analyzed simultaneously. To achieve that, the standard deviation of the spectral power (SDSP) along the slow-time dimension is extracted, as shown in the following equation:

$$\mathrm{SDSP}(\sigma r) = \sqrt{\frac{\sum_{r=1}^{R} (\boldsymbol{R}(m, r) - \mu_{\mathrm{s}}(r))^2}{N_{\mathrm{c}}}} \tag{1}$$

where $r = [1, 2, 3, \ldots, R]$ is the index corresponding to the range bins, μ_{s} is a vector with the mean of $\mathbf{R}(m, r)$ extracted along the slow time, and N_{c} is the number of chirps.

Since the movements of interest are being performed at a stationary range or with a slight range variation in the case of jump rope, the SDSP can easily differentiate the signatures corresponding to exercises from static clutter. The reason for that is because the exercises will have a high variation in spectral power over time at the range of the movement, and the static clutter will not have a considerable variation to be selected as an exercise. Depending on how close and at which angle relative to a static clutter the exercise is being performed, a high SDSP value at the range of the clutter might appear due to the movement of the exercise. However, the SDSP at the range of the clutter is smaller than an actual exercise and presents less range migration than the exercises. Given that the movements will have a higher SDSP than static objects and from moving clutters like a human subject walking behind the experiment, since the range of the moving clutter will change considerably over time, and the exercises are being performed at the same group of range bins, the moving clutter will not interfere in the SDSP enough to be considered as a new exercise [26], [27].

Since each exercise motion occupies more than one range bin, a group of range bins is selected for each target of interest. The threshold used for selecting the correct range bins for each exercise must be changed based on the distance between the radar and the respective targets of interest. The reason for that is because when an exercise is performed far away from the radar, it has a smaller RCS compared to the exercises performed close, as can be seen in the example in Fig. 4. Threshold 1 select the ranges of the first two exercises performed at 1 and 2 m away from the radar, respectively. Threshold 2 determines the ranges for the third exercise performed at 4 m away from the radar.

Finally, after choosing all range bins with a higher SDSP than the calculated thresholds, the selected range bins are divided into groups based on a range threshold. This range threshold should be less than the minimum distance between two exercises among all tests. If the distance between selected range bins is higher than the range threshold, then both sets of range bins are considered associated with different people

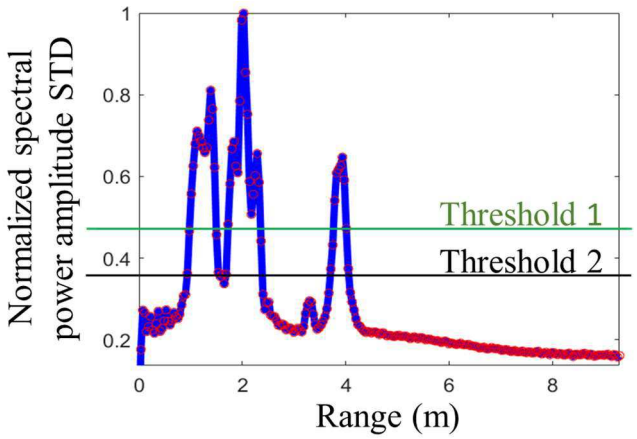

Fig. 4. Example of SDSP for three people doing exercises in front of an mmWave radar. Different thresholds for range selection are calculated when the exercises are performed from a longer distance.

doing exercises. The goal is to divide the group of ranges into the number of exercises performed. Finally, a matrix $\mathbf{E}(m, r_n)$ is created for each exercise, where r_n is the range bins for a single physical activity. Depending on how close the exercises are being performed to each other, the range resolution can be decreased by increasing the transmitted signal's bandwidth. As demonstrated in the following equation:

$$R_{\mathrm{res}} = \frac{C}{2 \times B} \tag{2}$$

where C is the speed of light and B is the bandwidth of the transmitted signal.

Succeeding the selection of the range bins with higher SDSP for each exercise, a short-time Fourier transform (STFT) is applied to the range bin with the highest spectral power among the ranges of each exercise. As shown in the following equation:

$$\mathrm{STFT}(t, \omega) = \sum_{m=0}^{M-1} \boldsymbol{E}(m, \mathrm{Mr}_n) w(m - t) e^{-\frac{j2\pi m\omega}{M}} \tag{3}$$

where $t = [1, 2, 3, \ldots, T]$ and $\omega = [1, 2, 3, \ldots, W]$ are the spectrogram's time and Doppler index, Mr_n is the range bin with maximum spectrum power for one exercise, and $w(t)$ is the chosen window function.

By doing that, it is possible to extract the mD signatures among the selected ranges. With this, the spectrogram is generated, thus producing essential features for classification.

C. Feature Extraction From mD Signatures

After the spectrogram generation, features for classification are extracted as shown in Fig. 5 and depicted as follows.

1) *Envelope:* The envelope was divided into two parts, the upper and lower envelope. The maximum power in each range bin was extracted to obtain both envelopes. In the analysis, frequencies extremely close to 0 Hz were removed since it represents static objects, and the analysis should focus on the movements. To avoid situations where the RCS of the movement is close to

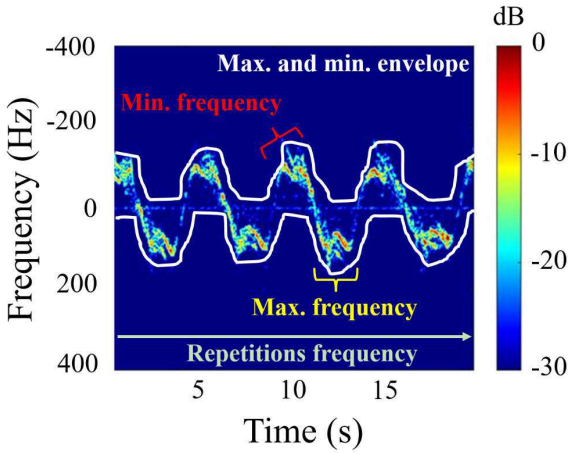

Fig. 5. Features extracted from the spectrogram analysis. (In the example, the mD signatures are from four sit-ups.)

zero and the maximum power point is outside the mD signature of the movement, a threshold of minimum power was established. If the value is smaller than the threshold, it is considered zero. That way, the envelope can be extracted.

2) *Minimum and Maximum Frequency:* It is the maximum and minimum frequency of the movements, which depends on the speed of the exercise motion.
3) *Repetitions Frequency:* It is the frequency of repetitions of the exercises. Since the exercises were recorded in a predetermined time and more than one repetition was performed in each data extraction, the repetition frequency helps differentiate exercises that, although they might have a high frequency in part of the motion, require more or less time to complete.
4) *Range:* Based on the previous range selection, the distance from the movement to the radar is also used as a feature. Since multiple experiments were performed, the same exercise is carried out at different ranges.

Based on the spectrogram information, the number of repetitions for each exercise can also be extracted. However, this information is not used as a feature and is more relevant when analyzing the user's performance.

D. Feature Extraction From Range–Doppler Frames

To further improve the classification, range–Doppler frames created by applying an FFT with a sliding window to the slow-time direction of the matrix were also analyzed. To extract the Doppler trajectory between frames for each separate movement, the same range bins selected using the SDSP previously are chosen. The matrix generated at each frame is sorted out into those range bins, thus generating a new matrix according to the number of exercises performed in the experiment. The following equation shows how one range–Doppler frame is created:

$$F_n(f, r_n) = \sum_{m=1}^{L} \boldsymbol{E}(m, r_n) e^{-\frac{j2\pi mf}{L}} \tag{4}$$

where F_n corresponds to one frame, f corresponds to the frequency index, and L is the length of the time window.

After dividing the range–Doppler matrices into smaller matrices for each exercise, the range–Doppler trajectory can be extracted for each individual movement. To do that, submatrices are generated inside the $\boldsymbol{F_n}(f, r_n)$ matrix and summed. The submatrix with the maximum power sum is selected in each frame to create the trajectory points. The size of the submatrices changes depending on how many range bins the exercise occupies. The following equation shows the sum of submatrices in one frame to extract the maximum power point:

$$e_{1,1} = \sum_{j=1}^{S}\sum_{i=1}^{S} \boldsymbol{F_{n_{(i,j)}}}, \ldots, e_{n,n} = \sum_{j=1}^{S}\sum_{i=1}^{S} \boldsymbol{F_{n_{(F+i-S, R_n+j-S)}}} \tag{5}$$

where S is the size of the square submatrix $\boldsymbol{S_m}(s, s)$ that depends on the range occupied by the movement of the exercise, if the movement occupies a large scope of range bins, the submatrices are bigger. $e_{1,1}$ and $e_{n,n}$ represent the first and last elements of the generated matrix containing the sum of submatrices that will be compared to select the trajectory point, and F and R_n are the sizes of the $\boldsymbol{F_n}(f, r_n)$ range–Doppler matrix. The center of the submatrix with the highest power sum is chosen as the trajectory point.

This approach of selecting the submatrix with maximum power is used because depending on how close the people doing exercises are to each other, signatures associated with different exercises might appear in some of the range–Doppler frames, and this submatrix acts as a filter, selecting the correct point instead of possible interferences from a different exercise or other artifacts. By following the point with the maximum RCS at each frame for all exercises, information about the range, Doppler, spectral power, and time can be extracted for the maximum points in each frame. Since the spectrogram can only provide information about one range bin at a time, by analyzing the range–Doppler frames, it is possible to include time information in the analysis and generate new features such as range movement variation, which is the measure of how the point of maximum RCS changed range over the frames. An example of range movement variation of a sit-up is depicted in Fig. 6. The range movement variation is an important feature for classification because movements like sit-ups change their maximum power range constantly due to the motion of the exercise, and movements like squats and sit-ups, for example, change the maximum RCS range. However, the amplitude of range variation is much smaller.

Since the exercises are being performed at different ranges and illumination angles, the RCS will vary depending on that. Therefore, power-related features were not used because the same exercise performed at a different range and perspective relative to the radar will present a different value of RCS. Hence, they are not considered solid features for classification.

E. Classification

After feature extraction, the features were fed into machine learning classifiers from the classification learner tool in MATLAB R2021b, aiming to achieve the highest classification accuracy possible. There are plenty of classification algorithms that can be used to predict categories. However, five algorithms were studied in this work: decision trees, SVMs, neural

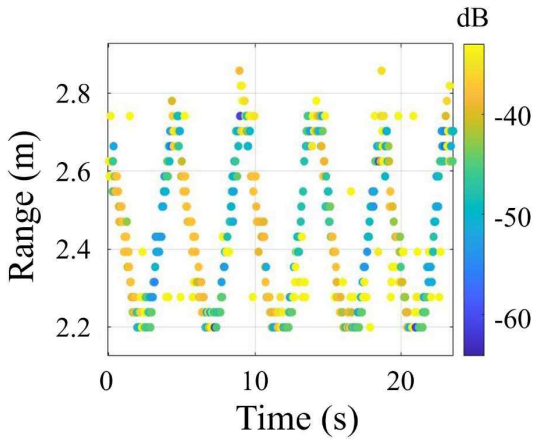

Fig. 6. Example of range movement variation of a sit-up at 3 m away from the radar (experiment number 8).

networks, naive Bayes, and ensemble. A brief introduction to the algorithms is depicted as follows.

1) *Decision Trees:* Decision tree learning is one of the most used predictive tools for decision-making. It can be used in different fields, such as statistical procedures, data mining, and machine learning. The decision tree structure is organized similar to a flowchart comparable to a tree, dividing the input into regions, where the top of the tree is called the root node, and the condition for decision-making is divided into branches that indicate a possible outcome or action. Finally, the tree's end, called the leaf node, provides the final predicted label [28].
2) *Support Vector Machine:* SVMs are one of the most powerful and robust algorithms for classification and regression in the most diverse fields of application. The SVM works by finding the best hyperplane between different data types in a multidimensional space, capable of best differentiating between features. The best hyperplane is the one that maximizes the margins separating categories in a gap that is as wide as possible. The new data are then classified based on which side of the gap they are in the same space [29], [30].
3) *Neural Network:* Neural networks, as the name suggests, are motivated by the learning process occurring in human brains to process information. Neural networks are organized on layers composed of interconnected nodes, similar to neurons. Those nodes contain an activation function that defines how the weighted sum of the input is transformed into an output. Following the schematic of a neural network, an input is fed to the network through the input layer, which further communicates it to one or more hidden layers, with every output being the input for a future function. The hidden layers perform all the processing and deliver the result to the output layer.
4) *Ensemble:* Ensemble is a machine learning system that combines a set of individual models working in parallel whose outputs are merged to obtain a better predictive performance. There are many types of ensembles. However, the main learning methods are bagging, stacking, and boosting [31].

To estimate the performance of the classification algorithms, the tenfold cross-validation method was used, where data are split into ten equal parts. The model's training is done in nine parts, and one subset is saved for testing. The process is repeated ten times, reserving a different tenth for testing until all parts have been tested. Finally, the accuracy obtained in all iterations is averaged to extract the model accuracy [32]. One advantage of this method is that it is not important how the data are split. Every data point appears in a test set exactly once and in a training set nine times. After feeding the features extracted to the machine learning algorithms, classification of the movements is achieved.

Even though all features are essential for the correct classification of the exercises, the following features play a major role in each exercise selection.

1) *Jump Rope:*
   a) *Repetition Frequency:* Jump rope is the fastest exercise among all exercises, with approximately two repetitions per second in most datasets.
   b) *Maximum and Minimum Frequencies:* Since the movement is fast, the maximum and minimum frequencies are always high.
2) *Sit-Ups:*
   a) *Range Variation:* Since the sit-up movement changes range over time, this feature helps differentiate sit-ups from other movements.
   b) *Repetition Frequency:* For most datasets, sit-ups had the smallest repetition frequency among the exercises since it takes more time to complete the movement than squats and push-ups.
3) *Push-Ups:*
   a) *Envelope:* By analyzing the envelope, it is possible to differentiate the mD signatures from this exercise from sit-ups and squats.
   b) *Maximum and Minimum Frequencies:* Since this movement consists of bending half of the arm, in most datasets, the maximum and minimum frequencies were the smallest.
4) *Squats:*
   a) *Envelope:* The envelope related to squats has strong signatures from the bending knee, differentiating it from other movements.

III. Experimental Results

To evaluate the effectiveness of the proposed approach, several experiments were conducted. The 1TX/3RX 60-GHz FMCW radar model BGT60TR13C by Infineon was employed during all the experiments. Although this radar system possesses one transmitting antenna and three receiving antennas, the baseband data obtained from only one transmitting antenna and one receiving antenna (one channel) were used in our analysis. The maximum unambiguous range using this radar is 15 m, and the maximum bandwidth is 5.5 GHz. The radar was placed 0.5 m above the ground for all experiments. Table I summarizes the information about all experiments done to validate the proposed approach. In Table I, "Exercise 1"

TABLE I
DETAILS OF THE EXPERIMENTAL SETUP AND DATASETS

N	Exercise 1	Distance 1 (m)	Exercise 2	Distance 2 (m)	Exercise 3	Distance 3 (m)	Additional interference	Qty of datasets
1	Push-ups	1	Sit-ups	3	-	-	Clutter at 3.5 m	5
2	Push-ups	1	Sit-ups	3	-	-	Clutter at 4.5 m	5
3	Push-ups	1	Sit-ups	3	-	-	Subject walking behind 1	5
4	Push-ups	1	Sit-ups	3	-	-	Subject walking behind 2	5
5	Push-ups	1	Sit-ups	3	Push-ups	5	-	5
6	Sit-ups	1	Push-ups	2	-	-	-	5
7	Sit-ups	1	Push-ups	3	-	-	-	6
8	Push-ups	1	Sit-ups	3	-	-	-	5
9	Sit-ups	1	Jump rope	2	-	-	-	5
10	Sit-ups	1	Jump rope	2	Squats	3	-	5
11	Squats	1	Jump rope	2	-	-	-	11
12	Sit-ups	1	Push-ups	2	Squats	4	-	5
13	Sit-ups	1	Squats	2	Push-ups	4	-	5
14	Jump rope	1	Squats	2	-	-	-	8
15	Push-ups	1	Squats	2	Jump rope	4	-	5
16	Squats	1	Jump rope	2	-	-	Clutter at 3 m	5
17	Jump rope	1	Squats	2	-	-	Clutter at 3 m	5
18	Push-ups	1	Sit-ups	2	Jump rope	4	-	5
19	Squats	1	Sit-ups	2	Jump rope	4	-	5
20	Squats	1	Sit-ups	2	Push-ups	4	-	5

TABLE II
FMCW RADAR PARAMETERS

Lower freq. (GHz)	60
Upper freq. (GHz)	61
Bandwidth (GHz)	1
Sample rate (kS/s)	2000
Range resolution (cm)	15
Chirp frequency (Hz)	806
Samples per chirp	128
Max. range (m)	9.6

column refers to the exercise performed by the person closer to the radar, and "Distance 1" is the distance from the person doing exercise 1 to the radar. "Exercise 2" is the exercise performed by another person in front of the radar simultaneous to exercise 1. "Distance 2" is the distance from the person doing exercise 2 to the radar. In some of the tests, three exercises were performed simultaneously in the radar's field of view. In those cases, "Exercise 3" column is the exercise done by the following person, and "Distance 3" is the distance from the person doing exercise 3 to the radar. Further information about the configuration used in the experiments can be found in Table II.

To validate the feasibility of the proposed solution in real scenarios, additional stationary and/or moving clutters were added to the analyzed scenarios. Large barrels were added to the radar's field of view to create stationary clutters to simulate objects such as wall pillars and furniture that a typical environment might have. For moving clutters, a human subject walked behind the targets of interest (while they were doing exercises) from two different initial points. In the first moving clutter experiment (experiment number 3), the subject walked from 10 to 5 m away from the radar. In Table I, this interference is named "Subject walking behind 1." In the second moving clutter experiment, the subject was 5 m away from the radar and walked at a trajectory similar to the azimuth angle, having the radar as a reference (experiment number 4). This interference is named "Subject walking behind 2." In those cases, the column "Additional interference" reports the type of interference, which is moving or stationary interferences.

The exercises were performed at different angles and ranges in front of the radar. In that way, all the targets of interest would always be illuminated by the radar's signals. Since the range resolution is 15 cm and the minimal distance between exercises is 1 m, the mD signatures of the exercises can be successfully retrieved. Table III illustrates the characteristics of the human subjects that contributed to the experiments. The volunteers were asked to perform exercises as they would in an actual working out scenario at a predetermined range and to perform the exercise at a predetermined time duration. Since the recording had a predetermined time, subjects carried out a different number of repetitions depending on their familiarity with the exercise. It is worth noting that some of the volunteers were not used to exercising regularly. To improve generalization even more, data from more human subjects could be added since people exercise in diverse ways.

In total, 20 types of tests were performed, 110 datasets were collected, and since more than one exercise was performed in each test, 260 exercises were recorded. Figs. 7–10 depict examples of the experiments carried out and the mD signatures of each exercise. Since people do exercises differently, some characteristics, such as the repetition frequency and maximum and minimum frequency, will vary depending on the subject that performed the movement. For the classification, the exercises were not divided by range or angle, so exercises like push-ups, for example, were analyzed at 1, 2, 3, 4, and 5 m away from the radar and at different angles. This makes the

TABLE III
INFORMATION OF THE VOLUNTEERS

Subject number	Gender	Height (m)	Weight (kg)
1	Male	1.88	85
2	Male	1.81	65
3	Male	1.85	82
4	Male	1.87	100
5	Male	1.70	63
6	Female	1.56	55
7	Female	1.60	51

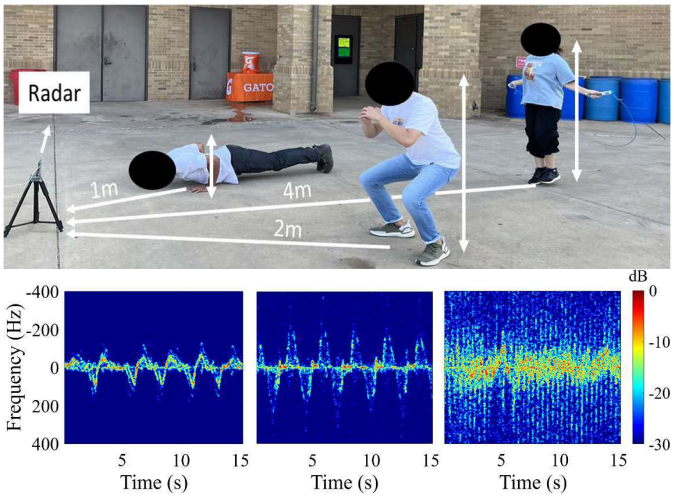

Fig. 7. Example of experiment number 15, and the mD signatures extracted.

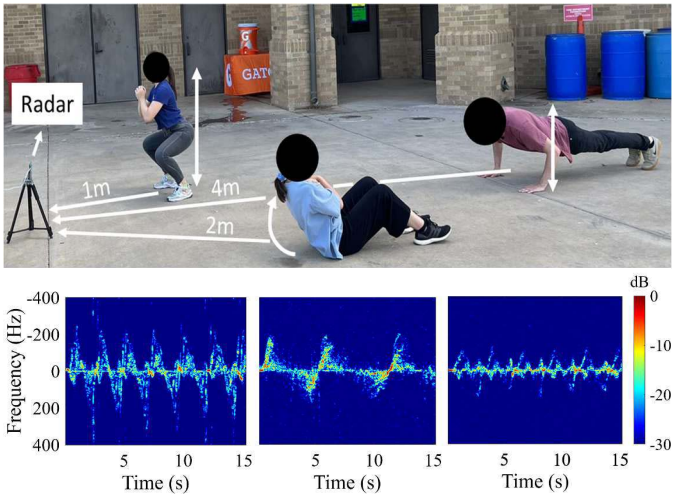

Fig. 8. Example of experiment number 20, and the mD signatures extracted.

classification harder since, depending on the range and angle, the exercise will occupy a different number of range bins and have different RCS.

Fig. 11 shows the accuracy of the algorithms used. Some of the SVM algorithms achieved the accuracy higher than 90%, whereas the quadratic SVM achieved the best classification results. Fig. 12 exhibits the confusion matrix of the quadratic SVM classification with tenfold cross-validation. The image also shows the true positive rate (TPR) of each exercise.

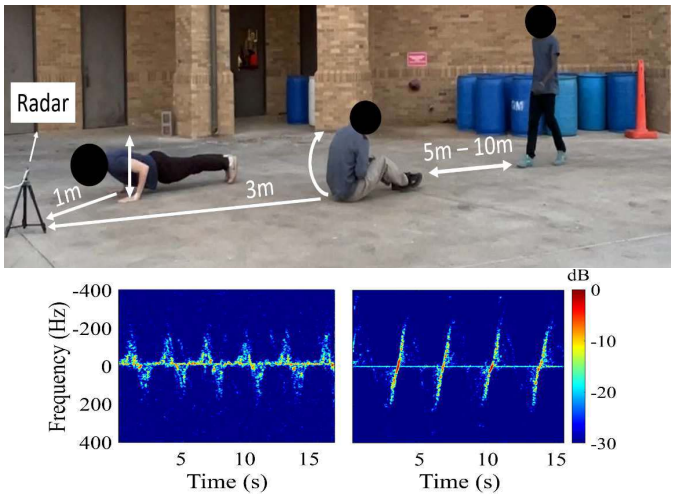

Fig. 9. Example of experiment number 3, and the mD signatures extracted.

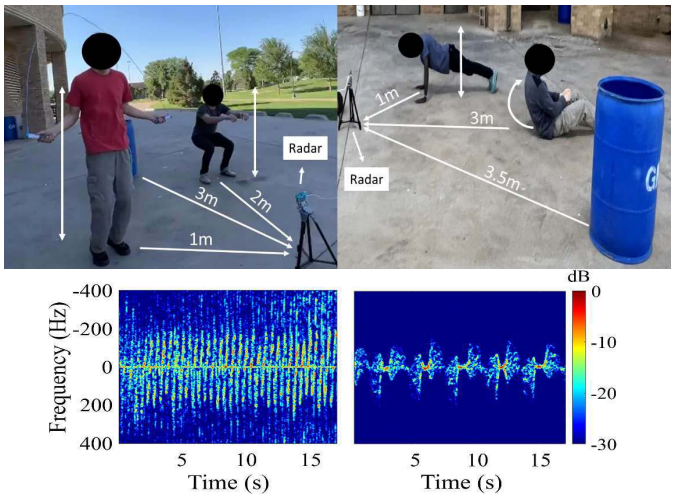

Fig. 10. Example of experiments 17 and 1, respectively, and the mD signatures extracted from experiment 17.

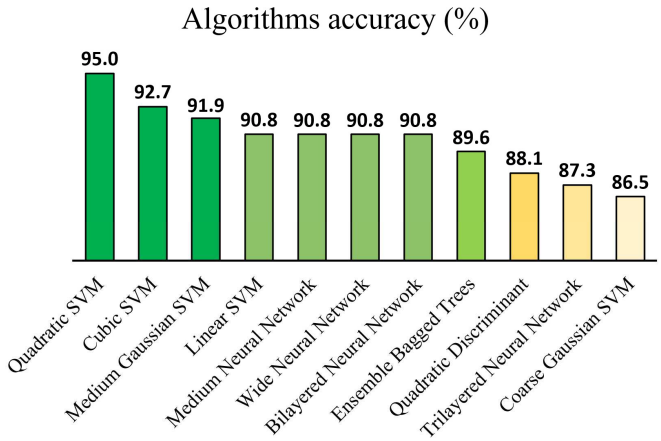

Fig. 11. Classification algorithms' accuracy with tenfold cross-validation.

For the sake of comparison, Table IV shows the contrast between this work with similar works that use FMCW radars to classify human motion, and presents information about the type of data used as input for classification, the maximum number of targets for one dataset, the number of channels of

TABLE IV
COMPARISON WITH SIMILAR WORKS

Reference	Type of sensor	Type of input	Max. simultaneous targets	Qty. of channels	Classification accuracy	Type of Clutter	Type of experiment	Number of volunteers
[21]	FMCW Radar	mD signatures, angle analysis	Two	Multiple channels	≈ 80%	Stationary	Human behavior detection	2
[39]	FMCW Radar	mD signatures	One	Single channel	85% and 96%	Stationary	Human behavior detection	99
[14]	FMCW Radar	Range Doppler, mD signatures	One	Single channel	94.8% and 93.3%	Stationary	Human behavior detection	6
[24]	FMCW Radar	Range Doppler, Range angle, angle-Doppler	One	Multiple channels	93% and 99.85%	Stationary	Exercises monitoring	2
This work	FMCW Radar	Range Doppler, mD signatures	**Three**	**Single channel**	95%	**Moving and stationary**	Exercises monitoring	7

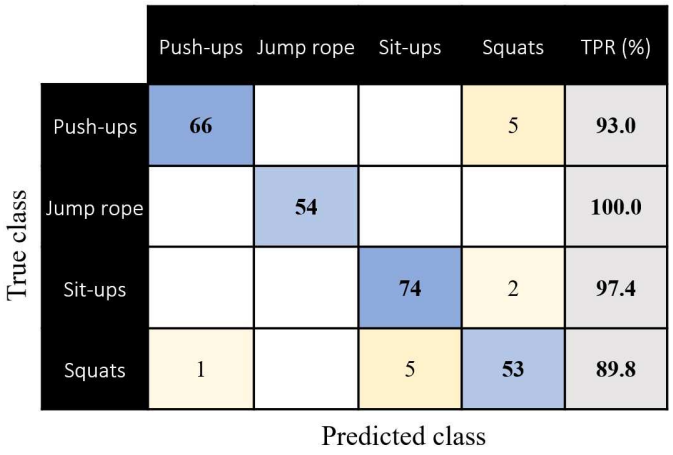

Fig. 12. Confusion matrix and TPR using quadratic SVM with tenfold cross-validation.

the radar used in the experiments, classification accuracy, and types of interferences.

IV. CONCLUSION

This article presented a novel multitarget exercise monitoring processing technique that works in different types of environments with moving and stationary clutter. The technique does not require multiple antennas that generate angular information, bringing a solution in a simple setup. The experiments were held out in 20 different scenarios, with more than one exercise being performed as the target of interest using the 60-GHz FMCW radar model BGT60TR13C by Infineon. The bandwidth used for the experiments was 1 GHz with a range resolution of 15 cm. The features from the exercises were extracted using mD analysis and range–Doppler frames and later used for classification. Four exercises were studied, i.e., push-ups, sit-ups, squats, and jump rope. To measure performance, counting the number of repetitions of each exercise is also possible using spectrogram analysis. After the experiments and feature extraction, a classification accuracy of 95% was achieved using quadratic SVM with tenfold cross-validation. Future works will investigate the feasibility of extracting mD information for multiple exercises performed at the same range using beamforming. Also, features related to the azimuth and elevation angles will be extracted and analyzed.

REFERENCES

[1] *Global Health Risks: Mortality and Burden of Disease Attributable to Selected Major Risks*, World Health Organization, Geneva, Switzerland, 2010.
[2] P. Slade, M. J. Kochenderfer, S. L. Delp, and S. H. Collins, "Sensing leg movement enhances wearable monitoring of energy expenditure," *Nature Commun.*, vol. 12, no. 1, p. 4312, Jul. 2021.
[3] W. Wang, B. Balmaekers, and G. de Haan, "Quality metric for camera-based pulse rate monitoring in fitness exercise," in *Proc. IEEE Int. Conf. Image Process. (ICIP)*, Sep. 2016, pp. 2430–2434.
[4] Z. Liu, X. Liu, and K. Li, "Deeper exercise monitoring for smart gym using fused RFID and CV data," in *Proc. IEEE INFOCOM Conf. Comput. Commun.*, Jul. 2020, pp. 11–19.
[5] G. Marta et al., "Wearable biofeedback suit to promote and monitor aquatic exercises: A feasibility study," *IEEE Trans. Instrum. Meas.*, vol. 69, no. 4, pp. 1219–1231, Apr. 2020.
[6] S. Garcia-de-Villa, A. Jimenez-Martin, and J. J. Garcia-Dominguez, "Novel IMU-based adaptive estimator of the center of rotation of joints for movement analysis," *IEEE Trans. Instrum. Meas.*, vol. 70, pp. 1–11, 2021.
[7] C. Li et al., "A review on recent progress of portable short-range noncontact microwave radar systems," *IEEE Trans. Microw. Theory Techn.*, vol. 65, no. 5, pp. 1692–1706, May 2017.
[8] Z. Li, A. Haigh, C. Soutis, A. Gibson, and P. Wang, "A review of microwave testing of glass fibre-reinforced polymer composites," *Nondestruct. Test. Eval.*, vol. 34, no. 4, pp. 429–458, Apr. 2019.
[9] H.-S. Lim, J. Jung, J.-E. Lee, H.-M. Park, and S. Lee, "DNN-based human face classification using 61 GHz FMCW radar sensor," *IEEE Sensors J.*, vol. 20, no. 20, pp. 12217–12224, Oct. 2020.
[10] Y. Li, Z. Peng, R. Pal, and C. Li, "Potential active shooter detection based on radar micro-doppler and range-Doppler analysis using artificial neural network," *IEEE Sensors J.*, vol. 19, no. 3, pp. 1052–1063, Feb. 2019.
[11] S. Lee, Y.-J. Yoon, J.-E. Lee, and S.-C. Kim, "Human-vehicle classification using feature-based SVM in 77-GHz automotive FMCW radar," *IET Radar, Sonar Navigat.*, vol. 11, no. 10, pp. 1589–1596, Oct. 2017.
[12] D. Rodrigues and C. Li, "Hand gesture recognition using FMCW radar in multi-person scenario," in *Proc. IEEE Topical Conf. Wireless Sensors Sensor Netw. (WiSNeT)*, Jan. 2021, pp. 50–52.
[13] Z. Peng, J.-M. Munoz-Ferreras, R. Gomez-Garcia, and C. Li, "FMCW radar fall detection based on ISAR processing utilizing the properties of RCS, range, and Doppler," in *IEEE MTT-S Int. Microw. Symp. Dig.*, May 2016, pp. 1–3.

[14] C. Ding et al., "Inattentive driving behavior detection based on portable FMCW radar," *IEEE Trans. Microw. Theory Techn.*, vol. 67, no. 10, pp. 4031–4041, Oct. 2019.

[15] Y. Ma et al., "Multitarget time-varying vocal folds vibration detection using MIMO FMCW radar," *IEEE Trans. Instrum. Meas.*, vol. 71, pp. 1–12, 2022.

[16] S. Miyahara, "New algorithm for multiple object detection in FM-CW radar," in *Intelligent Vehicle Initiative (IVI) Technology*. 2004, pp. 17–22.

[17] E. Hyun and J.-H. Lee, "A meothod for multi-target range and velocity detection in automotive FMCW radar," in *Proc. 12th Int. IEEE Conf. Intell. Transp. Syst.*, Oct. 2009, pp. 7–11.

[18] E. Hyun, W. Oh, and J.-H. Lee, "Multi-target detection algorithm for FMCW radar," in *Proc. IEEE Radar Conf.*, May 2012, pp. 338–341.

[19] Y. Fan, Z. Yang, X. Bu, and J. An, "Radar waveform design and multi-target detection in vehicular applications," in *Proc. Int. Conf. Estimation, Detection Inf. Fusion (ICEDIF)*, Jan. 2015, pp. 286–289.

[20] H. Liang, P. Wang, and X. Wang, "Simultaneous tracking of multiple targets using interferometric FMCW radar," in *Proc. IEEE Int. Conf. Signal, Inf. Data Process. (ICSIDP)*, Dec. 2019, pp. 1–6.

[21] F. Jin et al., "Multiple patients behavior detection in real-time using mmWave radar and deep CNNs," in *Proc. IEEE Radar Conf. (RadarConf)*, Apr. 2019, pp. 1–6.

[22] A. Hussain, K. Zafar, A. R. Baig, R. Almakki, L. AlSuwaidan, and S. Khan, "Sensor-based gym physical exercise recognition: Data acquisition and experiments," *Sensors*, vol. 22, no. 7, p. 2489, Mar. 2022.

[23] X. Guo, J. Liu, C. Shi, H. Liu, Y. Chen, and M. C. Chuah, "Device-free personalized fitness assistant using WiFi," in *Proc. ACM Interact., Mobile, Wearable Ubiquitous Technol.*, 2018, pp. 1–23.

[24] G. Tiwari and S. Gupta, "An mmWave radar based real-time contactless fitness tracker using deep CNNs," *IEEE Sensors J.*, vol. 21, no. 15, pp. 17262–17270, Aug. 2021.

[25] D. V. Q. Rodrigues and C. Li, "Noncontact exercise monitoring in multi-person scenario with frequency-modulated continuous-wave radar," in *IEEE MTT-S Int. Microw. Symp. Dig.*, Dec. 2020, pp. 1–3.

[26] V. G. R. Varela, D. V. Q. Rodrigues, and C. Li, "Separation of simultaneous multi-person noncontact physical activity signals using frequency-modulated continuous-wave radars," in *Proc. IEEE Topical Conf. Wireless Sensors Sensor Netw. (WiSNeT)*, Jan. 2022, pp. 5–7.

[27] Z. Peng et al., "A portable FMCW interferometry radar with programmable low-IF architecture for localization, ISAR imaging, and vital sign tracking," *IEEE Trans. Microw. Theory Techn.*, vol. 65, no. 4, pp. 1334–1344, Apr. 2017.

[28] A. Navada, A. N. Ansari, S. Patil, and B. A. Sonkamble, "Overview of use of decision tree algorithms in machine learning," in *Proc. IEEE Control Syst. Graduate Res. Colloq.*, Jun. 2011, pp. 37–42.

[29] N. Cristianini and J. Shawe-Taylor, *An Introduction to Support Vector Machines and Other Kernel-based Learning Methods*. Cambridge, U.K.: Cambridge Univ. Press, 2000.

[30] J. Cervantes, F. Garcia-Lamont, L. Rodríguez-Mazahua, and A. Lopez, "A comprehensive survey on support vector machine classification: Applications, challenges and trends," *Neurocomputing*, vol. 408, pp. 189–215, Sep. 2020.

[31] F. Huang, G. Xie, and R. Xiao, "Research on ensemble learning," in *Proc. Int. Conf. Artif. Intell. Comput. Intell.*, 2009, pp. 249–252.

[32] T.-T. Wong, "Performance evaluation of classification algorithms by K-fold and leave-one-out cross validation," *Pattern Recognit.*, vol. 48, no. 9, pp. 2839–2846, 2015.

[33] K. T. Olutomilayo, M. Bahramgiri, S. Nooshabadi, and D. R. Fuhrmann, "Extrinsic calibration of radar Mount position and orientation with multiple target configurations," *IEEE Trans. Instrum. Meas.*, vol. 70, pp. 1–13, 2021.

[34] Z. Zhang, X. Wang, D. Huang, X. Fang, M. Zhou, and Y. Zhang, "MRPT: Millimeter-wave radar-based pedestrian trajectory tracking for autonomous urban driving," *IEEE Trans. Instrum. Meas.*, vol. 71, pp. 1–17, 2022.

[35] C. Ding et al., "Continuous human motion recognition with a dynamic range-Doppler trajectory method based on FMCW radar," *IEEE Trans. Geosci. Remote Sens.*, vol. 57, no. 9, pp. 6821–6831, Sep. 2019.

[36] Y.-C. Chou, B.-Y. Ye, H.-R. Chen, and Y.-H. Lin, "A real-time and non-contact pulse rate measurement system on fitness equipment," *IEEE Trans. Instrum. Meas.*, vol. 71, pp. 1–11, 2022.

[37] S. Z. Gurbuz and M. G. Amin, "Radar-based human-motion recognition with deep learning: Promising applications for indoor monitoring," *IEEE Signal Process. Mag.*, vol. 36, no. 4, pp. 16–28, Jul. 2019.

[38] E. Sardini, M. Serpelloni, and V. Pasqui, "Wireless wearable T-shirt for posture monitoring during rehabilitation exercises," *IEEE Trans. Instrum. Meas.*, vol. 64, no. 2, pp. 439–448, Feb. 2015.

[39] U. Saeed et al., "Discrete human activity recognition and fall detection by combining FMCW RADAR data of heterogeneous environments for independent assistive living," *Electronics*, vol. 10, no. 18, p. 2237, Sep. 2021.

Victor G. Rizzi Varela (Graduate Student Member, IEEE) received the B.S. degree in electronics and telecommunications engineering from Mackenzie Presbyterian University, São Paulo, Brazil, in 2019. He is currently pursuing the Ph.D. degree in electrical engineering with Texas Tech University, Lubbock, TX, USA.

He joined Texas Tech University, in 2021, as a Research Assistant. His current research interests include biomedical applications of microwave/RF, microwave/millimeter-wave circuits and systems, and wireless sensors.

Davi V. Q. Rodrigues (Graduate Student Member, IEEE) received the B.S. degree in communications engineering from the Military Institute of Engineering, Rio de Janeiro, Brazil, in 2017. He is currently pursuing the Ph.D. degree in electrical engineering with Texas Tech University, Lubbock, TX, USA.

He joined Texas Tech University, in 2018, as a Research Assistant. In 2021, he joined Uhnder Inc., Austin, TX, where he was involved in the design and evaluation of signal processing algorithms for mitigation of radar interference. In 2022, he joined the Abbott Laboratories, Los Angeles, CA, USA, where he worked on the design of antennas and microwave systems for implantable medical devices. In 2022, he conducted research on wireless networks assisted by intelligent reflective surfaces with the Advanced Wireless Research and Development Group, Office of the CTO, Dell Technologies, TX. His current research interests include signal processing for radar and communication systems, wireless sensors for smart living and biomedical applications, and microwave/millimeter-wave circuits.

Mr. Rodrigues was a recipient of the Best Student Paper Award of the 2020 IEEE MTT-S International Microwave Biomedical Conference (IMBioC), the Best Paper Award—Antennas Category of the 2020 IEEE MTT-S Asia–Pacific Microwave Conference (APMC), the Best Student Paper Award—Honorable Mention of the 2021 IEEE MTT-S International Wireless Symposium (IWS), and the prestigious IEEE MTT-S Tom Brazil Graduate Fellowship Award in 2022.

Leya Zeng (Graduate Student Member, IEEE) received the B.S. and M.S. degrees in electrical engineering from the University of California at Riverside, Riverside, CA, USA, in 2020 and 2021, respectively. He is currently pursuing the Ph.D. degree in electrical engineering with Texas Tech University, Lubbock, TX, USA.

His current research interests include wireless RF sensing and detection, signal processing, and their applications.

Changzhi Li (Senior Member, IEEE) received the B.S. degree in electrical engineering from Zhejiang University, Hangzhou, China, in 2004, and the Ph.D. degree in electrical engineering from the University of Florida, Gainesville, FL, USA, in 2009.

He is currently a Professor with Texas Tech University, Lubbock, TX, USA. His research interests include microwave/millimeter-wave sensing for healthcare, security, energy efficiency, structural monitoring, and human–machine interface.

Dr. Li is an IEEE Microwave Theory and Techniques Society (MTT-S) Distinguished Microwave Lecturer, in the Tatsuo Itoh class of 2022–2024. He was a recipient of the IEEE MTT-S Outstanding Young Engineer Award, the IEEE Sensors Council Early Career Technical Achievement Award, the ASEE Frederick Emmons Terman Award, the IEEE-HKN Outstanding Young Professional Award, and the NSF Faculty Early CAREER Award. He is an Associate Editor of the IEEE JOURNAL OF ELECTROMAGNETICS, RF AND MICROWAVES IN MEDICINE AND BIOLOGY.